Memorias del Congreso Nacional de Control Automático
ISSN: 2594-2492

Optimal Control of Make - up Lubricating Systems for Internal Combustion Engines

Saúl Domínguez-García*, Luis Béjar-Gómez, Fabricio Nápoles-Rivera***, Rafael Maya-Yescas******

Universidad Michoacana de San Nicolás de Hidalgo, 58030, Morelia, Michoacán de Ocampo, México
** Facultad de Ingeniería Mecánica (e-mail: sdominguez@umich.mx)*
*** Facultad de Ingeniería Mecánica (e-mail: luis.bejar@umich.mx)*
**** Facultad de Ingeniería Química (e-mail: fabricio.napoles@umich.mx)*
**** Facultad de Ingeniería Química (e-mail: rafael.maya.yescas@umich.mx)*

ABSTRACT: This research deals with the optimal control of make-up lubricating systems for internal combustion engines. Firstly, classic mass balances are proposed to depict the dynamics of the width of the tribological film protecting the rubbing surfaces; this is a competitive "renovation-removal" process that can reach optimal steady state. Secondly, to regulate the film width in this steady state, optimal trajectories of make-up of lubricant in the engine's oil pan and supply of lubricant from the oil pan to the engine are deduced using optimal control methodology. Results show feasible tracks to be followed by lubricating system to reach the optimal steady state, which simultaneously minimize the lubricant consumption.

Keywords: Dynamics, Engine, Lubricants, Optimal control, Optimal trajectory.

1. INTRODUCTION

1.1. Physical Model: The Engine

Lubricating systems are the main responsible avoiding the deterioration of mechanical devices and preserving the energy efficiency of engines. In general, lubrication is provided by a protective tribofilm (Fig. 1a), which is generated by reactions of lubricant precursors. During engine operation the tribofilm suffers removal, then debris and waste products are accumulated in the lubricant blend; these wastes do not rub surfaces. Hence, the optimal functioning of the lubricating system is the main target during the engines operating time. The mechanistic generation and removal of tribofilms in internal combustion engines have been modelled employing first order reaction rates (see Appendix A), incorporating them in the classic mass balances for the lubricant precursors, the tribofilm and the waste (Domínguez-García et al., 2020).

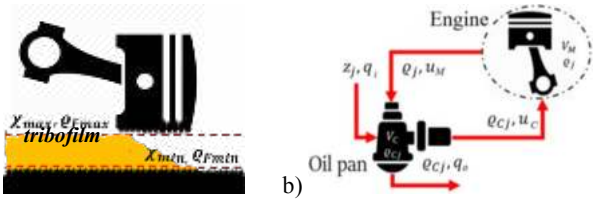

a) b)

Figure 1. Schematics of the System under Study. a) Detail of the tribofilm, b) the "engine-oil pan" system.

This engine (Fig. 1b) is characterized by its fix volume V_M; it receives lubricant from the oil pan, at volumetric rate u_C, and returns the lubricant to the oil pan at volumetric rate u_M, after it was used. The oil pan, which is characterized by its fix volume V_C, fresh lubricant is supplied as "make-up", at volumetric rate q_i and from which is purged at volumetric rate q_o. Composition is different in each one of the streams, characterized by mass fraction of the '*j-th* compound' ρ_j.

The mass balances follow tribofilm precursors '*A*', which reacts to form the tribofilm present on the surface of the rubbing surfaces '*F*', which is removed in form of debris '*D*' (1). To facilitate the handling of the lubricating system model and to force it to maintain a satisfactory tribofilm thickness throughout the operating time, the variable "excess of mass fraction of *A*" (θ_A) is introduced (2).

$$A \overset{\kappa_A}{\rightarrow} F \overset{\kappa_F}{\rightarrow} D \tag{1}$$

$$\theta_A = \rho_{CA} - \rho_{Ae} \tag{2}$$

Here, κ_A and κ_F are kinetic rate constants, ρ_{CA} is the mass fraction of *A* in the oil pan and ρ_{Ae} is that fraction of *A* inside the engine that holds the tribofilm, renovation and removal, rates balanced; as consequence, the mass fraction of *F* does not vary on the rubbing surfaces, maintaining the tribofilm thickness constant as the goal of the regulation process.

Considering the above settings, the system model is reduced to 2 equations; the first one describes the dynamics of the system state θ_A (3) and the second one constrains the state of the system to hold the tribofilm thickness (4).

$$\frac{d\theta_A}{dt} = -\frac{\kappa_A \rho_{ACe}}{V_C} + (z_A - \rho_{ACe} - \theta_A)\frac{q_i}{V_C} \tag{3}$$

$$0 = \theta_A u_M - \kappa_A \rho_{Ae} \tag{4}$$

Here, z_A is the mass fraction of *A* in fresh lubricant make-up. Details of the deduction of the equations (2) and (3) can be found in (Domínguez-García et al., 2020; 2021).

1.2. The steady states of the lubricating system

The value of the system state (θ_A) changes because of the balance between the excess of *A* within the oil pan vessel, which fulfils the fresh lubricant requirements, and the

competitive renovation-removal process, which depletes the excess of *A*. So, if the system is made-up with fresh lubricant, it just moves to a steady state that ensures excess of *A* does not deplete more. In these conditions $d\theta_A/dt = 0$; then mass balances (3) and (4) are fixed by two algebraic equations, (5) and (6); which relate q_i with θ_A and q_i with u_M.

$$\theta_A = z_A - \rho_{Ae} - \frac{\kappa_A \rho_{Ae}}{q_i} \tag{5}$$

$$u_M = \frac{\kappa_A \rho_{Ae}}{z_A - \rho_{Ae} - \frac{\kappa_A \rho_{Ae}}{q_i}} \tag{6}$$

1.3. The Optimal Control Problem

In order to optimize two objectives: a) minimizing the lubricant supplied to the oil pan, and b) maintaining the width of the lubricating tribofilm, in this work the set of mass balances (5, 6), which takes into account the dynamics of tribofilm thickness as function of chemical and mechanical processes, is tracked for optimal trajectories of make-up of lubricating in the engine's oil pan and supply of lubricant from the oil pan to the engine. This problem emerges from the fact that daily operation of the engine starts far from the optimal point, so it requires to be tracked until reaching the desired operating conditions. Additionally, changes in composition of the fresh lubricant can modify the optimal lubricant make-up, building a complex problem to solve.

2. METHODOLOGY

2.1. Problem Statement

Experimental results previously reported for tribofilm generation and removal, as well as the mass balances for a lubricating system for internal combustion engines (Domínguez-García, 2020; 2021), are taken as bases for this research. The system under consideration consists of the engine, which works as the chemical reactor where tribofilm is generated and removed, and the oil pan, which is the mixer of the lubricant streams coming from the engine (u_M) and the make-up (q_i). The target is to ensure width (Fig. 1a) to be between its maximum (χ_{Max}) and minimum (χ_{Min}) values (Fig. 1a) by forcing the excess of lubricant precursors (θ_A) the closest possible to its set point (7), the optimal fraction ($\theta_{A,Opt}$). The manipulating variables are the flows entering and leaving the engine, which for mechanical reasons, since V_M is the volume of a rigid vessel, should be of the same value (8), and the flows supplied to and removed from the oil pan, which should also be of the same value (9), since V_C is the volume of a rigid vessel.

$$\theta_A(t) \cong \theta_{A,Opt} \tag{7}$$

$$u_C(t) = u_M(t) \equiv u(t) \tag{8}$$

$$q_i(t) = q_o(t) \equiv q(t) \tag{9}$$

2.2. Finding the trade-off steady state

Firstly, a two objective optimization is carried out, considering the minimization of used and wasted lubricant $q(t)$ and simultaneously minimizing the rate of lubricant supply that is sent from the oil pan to the engine $u(t)$; the restrains to the optimization are the mass balances (3, 4) and the fact that the flows $q(t)$ and $u(t)$ have to be finite and inside a feasible operating window.

A quadratic performance index is used to ensure that the steady state found is a minimum point; the sum of the square of $q(t)$ and the square of $u(t)$ is a convex function, i.e. it has a global minimum point. Moreover, it is desired to reduce the consumption of lubricant during a period τ, so it is necessary to minimize the integral of the performance index with respect to time (10). A factor ½ is added to performance index to facilitate the algebraic procedure. Then, according to the optimal control methodology (Alekseev, 2013), the motion equation (Hamiltonian) for this optimization problem is built by adding the performance index (10) to the restrains imposed by mass balances (2, 3), and it is necessary to add one adjoined variable (Jacobi eq.) to each restriction (11).

$$Min\left\{\int_0^\tau \frac{1}{2}(q^2 + u^2)\, dt\right\} \tag{10}$$

$$H = \frac{1}{2}(q^2 + u^2) + \lambda\left[-\frac{\kappa_A \rho_{Ae}}{V_C} + (z_A - \rho_{Ae} - \theta_A)\frac{q}{V_C}\right] + \gamma(\theta_A u - \kappa_A \rho_{Ae}) \tag{11}$$

Here, H is the Hamiltonian functional, λ is the adjoined multiplier for restrain (3) and γ is the multiplier variable for restrain (4).

Once H is built, optimal point has to fulfill the necessary conditions for a static critical point, these conditions are the partial derivatives of H respect to state (12), adjoined multipliers (13, 14) and control variables (15-16) should be zero (Alekseev, 2013).

$$\frac{\partial H}{\partial \theta_A} = -\frac{\lambda q}{V_C} + \gamma u = 0 \tag{12}$$

$$\frac{\partial H}{\partial \lambda} = -\frac{\kappa_A \rho_{Ae}}{V_C} + (z_A - \rho_{Ae} - \theta_A)\frac{q}{V_C} = 0 \tag{13}$$

$$\frac{\partial H}{\partial \gamma} = \theta_A u - \kappa_A \rho_{Ae} = 0 \tag{14}$$

$$\frac{\partial H}{\partial u} = u + \gamma \theta_A = 0 \tag{15}$$

$$\frac{\partial H}{\partial q} = q + \frac{\lambda}{V_C}(z_A - \rho_{Ae} - \theta_A) = 0 \tag{16}$$

It should be highlighted that here a static critical point is sought to operate the lubricating system in the optimal steady state given by (7), embedded in (5, 6) and constrained by (3, 4), however for a static critical point it must be fulfilled that $d\theta_A/dt = 0$. In these conditions the dynamic optimal problem is simplified to a classical time invariant optimization problem and partial derivatives of *H* are nullified (Alekseev, 2013).

After a suitable algebraic labour, it is found that the optimal values of the state variable and control variables that fulfil necessary conditions (12-16) are (17) and (18). Although the values of the adjoined multipliers are not further necessary, those are presented just for completeness (19).

$$\theta_{A,Opt} = \frac{1}{2}(z_A - \rho_{Ae}) \tag{17}$$

$$u_{Opt} = q_{Opt} = 2\frac{\kappa_A \rho_{Ae}}{z_A - \rho_{Ae}} \tag{18}$$

$$\lambda = \gamma = -4\frac{V_C \kappa_A \rho_{Ae}}{(z_A - \rho_{Ae})^2} \tag{19}$$

2.3. Tracking the trade-off steady state

Now, following the methodology of optimal control relationships (Alekseev, 2013), the following functions are developed: deviation variables for the flow to and from the engine (20), deviation variables for the flow to and from the oil pan (21), deviation of excess of lubricant precursors (22).

$$\phi_u = u_{Opt} - u(t) \tag{20}$$

$$\phi_q = q_{Opt} - q(t) \tag{21}$$

$$\phi_A = \theta_{A,Opt} - \theta_A(t) \tag{22}$$

By combining equations (20-22) with mass balances (3, 4), restrains for the lubricating system are obtained as functions of the deviation variables (23, 24).

$$\frac{d\phi_A}{dt} = \frac{\kappa_A \rho_{Ae}}{V_C} - \frac{(\Lambda_{Opt} + \phi_A)(\phi_q - q_{Opt})}{V_C} \tag{23}$$

$$0 = (\theta_{A,Opt} - \phi_A)(u_{Opt} - \phi_u) - \kappa_A \rho_{Ae} \tag{24}$$

$$\Lambda_{Opt} = z_A - \rho_{Ae} - \theta_{A,Opt} \tag{25}$$

Here, Λ_{Opt} (25) is an auxiliary parameter that simplifies (23).

Now, the problem is stated as follows: Minimize the deviation of manipulate and control variables (20-22) to reach the optimal steady state (12-16) as soon as possible. Here again, to ensure that the tracks to the steady state are minimum paths, a quadratic performance index is used (26), which is a convex function, meaning that it has global minimum paths. Moreover, it is desired to reduce the deviation of state and control variables during a period τ, so it is necessary to minimize integral of the performance index in time (26).

$$Min\left\{\int_0^\tau \frac{1}{2}\left(R{\phi_A}^2 + {\phi_u}^2 + {\phi_q}^2\right) dt\right\} \tag{26}$$

Besides, the factors ½ and R are added to performance index to facilitate the algebraic procedure and to make all terms in performance index dimensionally homogenous. Then, the Hamiltonian for this optimization problem is built by adding the performance index (26) to the restrains imposed by mass balances (23, 24), and including one adjoined variable for each restriction (27). Here λ is the adjoined variable for restrain (23) and γ is the adjoined variable for restrain (24).

Once H is built, the optimal path has to fulfil the necessary conditions for a dynamic critical path; these conditions are the

$$\begin{aligned} H = {} & \frac{1}{2}\left(R{\phi_A}^2 + {\phi_u}^2 + {\phi_q}^2\right) \\ & + \lambda\left[\frac{\kappa_A \varrho_{Ae}}{V_C} - \frac{(\Lambda_{Opt} + \phi_A)(q_{Opt} - \phi_q)}{V_C}\right] \\ & + \gamma\left[(\theta_{A,Opt} - \phi_A)(u_{Opt} - \phi_u) - \kappa_A \rho_{Ae}\right] \end{aligned} \tag{27}$$

multipliers (29) and control variables (30-32). However, this occasion they are not equal to zero: the partial derivative of H respect to ϕ_A is equal to $-d\lambda/dt$, and the partial derivative of H respect to λ is equal to $d\phi_A/dt$.

$$\frac{\partial H}{\partial \phi_A} = R\phi_A + \lambda\frac{(q_{Opt} - \phi_q)}{V_C} - \gamma(u_{Opt} - \phi_u) = -\frac{d\lambda}{dt} \tag{28}$$

$$\frac{\partial H}{\partial \lambda} = \frac{\kappa_A \varrho_{Ae}}{V_C} - \frac{(\Lambda_{Opt} + \phi_A)(q_{Opt} - \phi_q)}{V_C} = \frac{d\phi_A}{dt} \tag{29}$$

$$\frac{\partial H}{\partial \gamma} = (\theta_{A,Opt} - \phi_A)(u_{Opt} - \phi_u) - \kappa_A \rho_{Ae} = 0 \tag{30}$$

$$\frac{\partial H}{\partial \phi_u} = \phi_u - \gamma(\theta_{A,Opt} - \phi_A) = 0 \tag{31}$$

$$\frac{\partial H}{\partial \phi_q} = \phi_q + \frac{\lambda(\Lambda_{Opt} + \phi_A)}{V_C} = 0 \tag{32}$$

It should be highlighted that here a tracking to the static critical point is sought to operate the lubricating system in the optimal steady state given by (7), embedded in (5, 6) and constrained by (3, 4) as soon as possible, however for the track to static critical point the term $d\theta_A/dt$ can lies from zero. In these conditions the derivatives of H with respect to the state produces the adjoin equations which are the dynamics of the Lagrange multiplier $-d\lambda/dt$ (Alekseev, 2013).

Now, since (28-32) cannot be analytically solved. Instead, using algebra and differential calculus, a pair of differential equations that relate the deviation state ϕ_A and the deviation control ϕ_q (33, 34) can be obtained.

$$\frac{d\phi_A}{dt} = \frac{\kappa_A \varrho_{Ae}}{V_C} - \frac{(\Lambda_{Opt} + \phi_A)(q_{Opt} - \phi_q)}{V_C} \tag{33}$$

$$\frac{d\phi_q}{dt} = \phi_q \frac{\kappa_A \varrho_{Ae}}{V_C(\Lambda_{Opt} + \phi_A)} + \psi\frac{(\Lambda_{Opt} + \phi_A)}{V_C} \tag{34}$$

$$\psi = -\frac{(\kappa_A \rho_{Ae})^2}{(\phi_A + \theta_{A,Opt})^3} + \frac{\kappa_A \rho_{Ae} u_{Opt}}{(\phi_A + \theta_{A,Opt})^2} - R\phi_A \tag{35}$$

$$\phi_u = u_{Opt} - \frac{\kappa_A \rho_{Ae}}{\theta_{A,Opt} - \phi_A} \tag{36}$$

Here, ψ (35) is an auxiliary variable that makes (34) simpler. Once tracks of ϕ_A and ϕ_q are computed, the missing deviation variable ϕ_u can be calculated off-line (36). By this moment, the values of the adjoined multipliers are not further necessary.

The mass balances and the optimal control problem were solved for 9 different cases, which combine low, middle, and high levels of initial deviation of lubricant precursors (ϕ_{A0}), {0.01, 0.05, 0.10} g/L respectively, and low, middle, and high levels of initial deviation of lubricant supply (ϕ_{q0}), {0.0, 0.5, 1.0} L/s respectively; these cases are described in Table 1.

Table 1. Deviation levels for cases under study.

ϕ_{q0} \ ϕ_{A0}	*Low*	*Middle*	*High*
Low	Case 1	Case 4	Case 7
Middle	Case 2	Case 5	Case 8
High	Case 3	Case 6	Case 9

3. RESULTS AND DISCUSSION

To simulate lubricating system and the tracks to trade-off steady state for the 9 cases given in Table 1, (33-36) were solved using RK4 methodology implemented in Matlab™. All simulation were carried out using $\rho_{Ae} = 5\ g/L$, $\kappa_A = 6.5 \times 10^{-5}\ L/s$, $z_A = 40\ g/L$ and $V_C = 2.5\ L$, which are common values in experimental test and simulations (Domínguez-García et al., 2020; 2021; Ma and Luo, 2016).

The results are shown in two parts: Firstly, location of optimal trade-off steady state point is computed and discussed in Section *A*. Secondly, the 9 study cases are discussed to analyse control tracks for different deviations from the optimal trade-off steady state point in Section *B*.

3.1. The optimal trade-off steady state

Prior to locate the optimal trade-off steady state, it is suitable to describe the behaviour of Pareto's curves. On the one hand, the profile relating q and θ_A (5, Fig. 2a) is an increasing asymptotic curve that begins at $\theta_A = 0\ g/L$ and $q = 9.14 \times 10^{-6} L/s$, and continues towards $\theta_A = 35\ g/L$. However, this maximum value is reached for $q = \infty\ L/s$; therefore, this extreme is unfeasible. On the other hand, Pareto's curve relating q and u (6, Fig. 2b) is a hyperbolic decreasing curve which is limited by two asymptotes, one vertical that is placed in $q = 9.14 \times 10^{-6}$ and another horizontal that placed in $u = 9.14 \times 10^{-6}$; it is a symmetric hyperbolic curve. However, reaching any one of these extreme levels is unfeasible because one of the flows, either $q(t)$ or $u(t)$, is infinite. Therefore, the lubricating system cannot operate under conditions of either minimum q or minimum u.

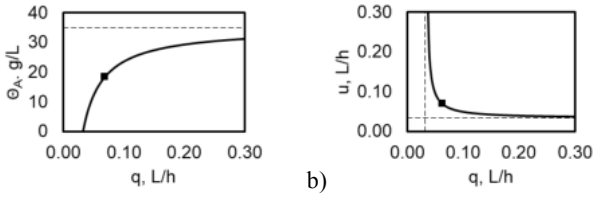

a) b)

Figure 2. Pareto's diagram showing the compromising relationship between flows q and u. the desired operating point is shown by the solid square. a) Manipulate input flow *versus* optimal mass fraction. b) Manipulate input flow *versus* engine flows.

Then, the first step of the methodology invokes compromising results, which are represented as a square mark in Pareto's diagram (Figs. 2a, 2b). After optimization, the point is found as the optimal trade-off steady state that locates the operating point, which demands feasible values of q and u (18): $\theta_{A,Opt} = 17.5\ g/L$ (16), $u_{Opt} = q_{Opt} = 1.83 \times 10^{-5} L/s$.

3.2. Tracks to trade-off steady state

Daily operation of the engine starts far from the trade-off optimal steady state point; therefore, it requires to be tracked until the desired operating conditions. Hence, to analyse tracks to the optimal point from the cases in Table 1, simulations use a weight factor $R = 10\ L^3/(g \cdot s^2)$. Results of this dynamic optimization problem are transversally addressed, i.e. the profile of each variable for nine cases is discusses in parallel.

Note that optimization is carried out solving equations (33-36) which are functions of deviation variables; in order to facilitate the understanding of the obtained results, (20-22) are used to compute the excess of lubricant precursors θ_A and the flows q and u in each case.

All simulations start considering excess of lubricant precursors θ_A; this excess in θ_A is established by the initial levels ϕ_A and goes toward $\theta_{A,Opt}$, however there are no important modifications of profiles caused by different levels of initial deviation of lubricant supply ϕ_q (Fig. 3).

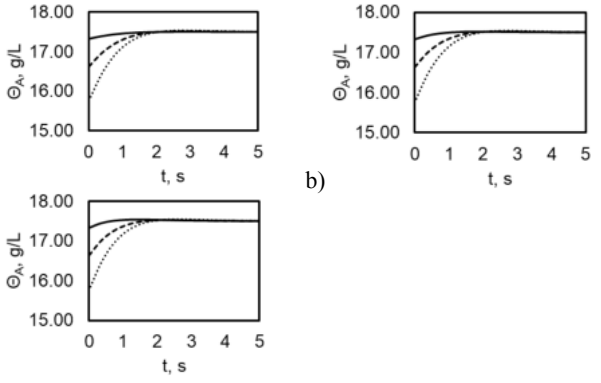

a) b) c)

Figure 3. Excess of lubricant precursors versus time. a) Low ϕ_q, Case 1 —, Case 2 --, Case 3. b) Middle ϕ_q, Case 4 —, Case 5 --, Case 6. c) High ϕ_q, Case 7 —, Case 8 --, Case 9.

These nine cases are illustrated in three groups: Cases 1-3 address with three levels of initial ϕ_A, low, middle, and high respectively, but all these three cases are simulated at the initial low level of ϕ_q (Fig. 3a). Cases 4-6 are grouped in the same way, but these three cases are simulated at the middle level of ϕ_q (Fig. 3b). Finally, cases 7-9 are also grouped in the same way, but these three cases are simulated at the high level of ϕ_q (Fig. 3c).

Since u is related to θ_A by the constrain (4), there are also no important modifications of profiles caused by different levels of initial deviation of lubricant supply ϕ_q (Fig. 4). At the beginning, all nine cases demand high levels of lubricant flow, therefore u goes toward u_{Opt}. It should be highlighted that if deviation of lubricant precursors is rather high, the mechanical system may not have the ability to supply precursors, which is an operating problem: Most of the removal on engines occurs

at the starting time, when pumps cannot send enough lubricant to the engine, so the protecting tribofilm decreases below its minimum level (Ma and Luo, 2016).

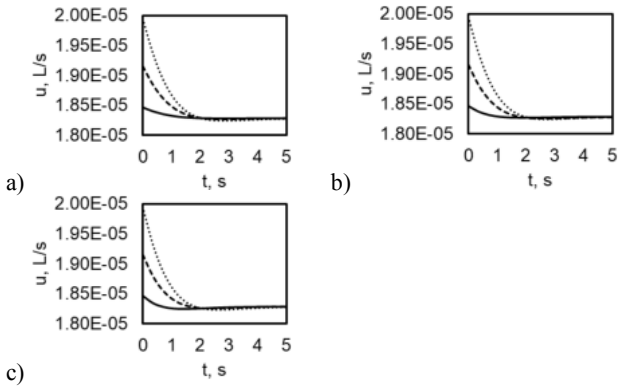

Figure 4. Lubricant flow sent to engine versus time. a) Low ϕ_q, Case 1 —, Case 2 --, Case 3. b) Middle ϕ_q, Case 4 —, Case 5 --, Case 6. c) High ϕ_q, Case 7 —, Case 8 --, Case 9.

Although profiles of excess of lubricant precursors θ_A and lubricant flow sent to engine u are not observably affected by initial deviation of lubricant supply ϕ_q, the profiles of lubricant supply q are modified. In all cases, when initial deviation of lubricant supply ϕ_q is low, flow q begins at low level fixed by ϕ_q, then there is an overshoot reaching a maximum point, and later all three cases go dawn towards q_{Opt} (Fig. 5a). The remaining cases behave similar; however, if deviation of lubricant precursors ϕ_A is low (cases 4, 7), profile of q does not increase, it just goes dawn towards q_{Opt} (Figs. 5b, 5c).

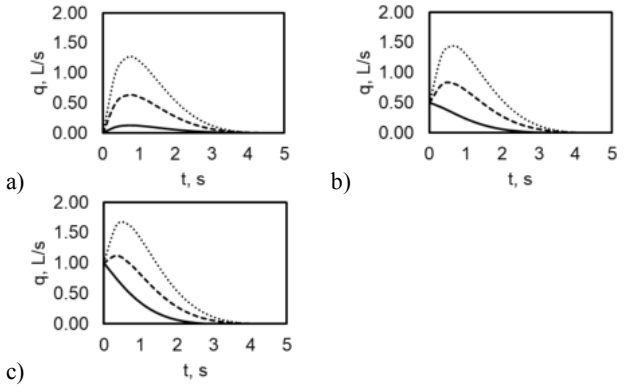

Figure 5. Lubricant supply flow versus time. a) Low ϕ_q, Case 1 —, Case 2 --, Case 3. b) Middle ϕ_q, Case 4 —, Case 5 --, Case 6. c) High ϕ_q, Case 7 —, Case 8 --, Case 9.

On the one hand, the overshoot behaviour provokes the system's state to move towards the steady state (Figs. 6a-6c). Physically, it is easy to understand that if the lubricating system is at low mass fraction of precursors, it is necessary supply a large amount of fresh lubricant; then q moves to a higher level, until the system have reached its new optimum level by supplying q_{Opt}.

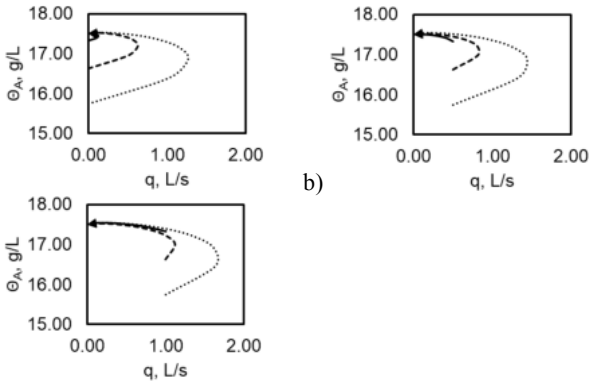

Figure 6. Pareto's curves of low level of lubricant precursors versus lubricant supply. a) Low ϕ_q, Case 1 —, Case 2 --, Case 3. b) Middle ϕ_q, Case 4 —, Case 5 --, Case 6. c) High ϕ_q, Case 7 —, Case 8 --, Case 9.

On the other hand, cases which only go dawn towards q_{Opt} indicate that deviation of lubricant supply is, at least, enough to carry the system to the desired steady state.Pareto's curves of the tracks to carry the lubricating system to the optimal steady state show, in all nine cases, elliptical trajectories (Fig. 7). This behaviour is caused because the optimal steady state is an attractor for the trajectories (Malcolm, 2007).

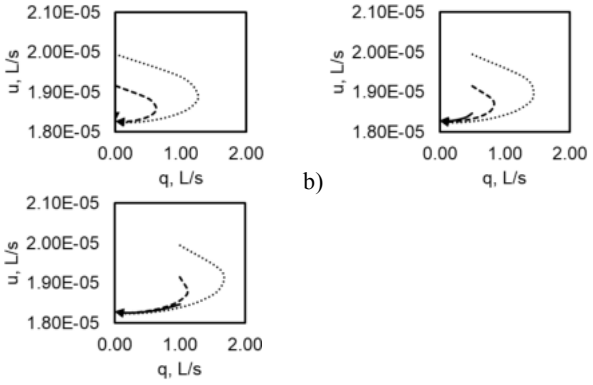

Figure 7. Pareto's curves of lubricant flow between oil pan and engine versus lubricant supply. a) Low ϕ_q, Case 1 —, Case 2 --, Case 3. b) Middle ϕ_q, Case 4 —, Case 5 --, Case 6. c) High ϕ_q, Case 7 —, Case 8 --, Case 9.

Note that, in cases where deviation of lubricant precursor ϕ_A is low and initial deviation of lubricant supply ϕ_q is high or middle, there is an unfavorable modification that makes tracks to steady state longer (Figs. 6b, 6c, 7b, 7c); this behaviour should consume more lubricant (Figs. 5b, 5c). Also note that, although in some profiles of lubricant supply and its profiles are larger, there is not important reduction of time to reach steady state (Figs. 5, 6).

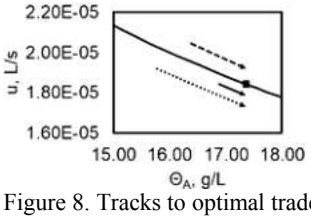

Figure 8. Tracks to optimal trade-off steady state.

Low ϕ_A —, Middle ϕ_A --, High ϕ_q; ▪ $\theta_{A,Op}$.

Finally, Pareto's curves that show the movement lubricating system state along excess of lubricant precursors θ_A and lubricant flow sent to engine u is very similar for low, middle and high deviation of lubricant supply ϕ_q, because constrain (4) has to be always satisfied; arrows (Fig. 8) show tracks from low, middle and high level from ϕ_A to $\theta_{A,Op}$.

Just for completeness, the results obtained after negative deviations of the optimal steady state are not presented in this document, since taking the system from a high level of excess lubricant precursors to a lower level requires nil flows, meaning "do nothing", just wait for the excess of lubricating precursors diminishes due to tribofilm removal.

The proposed procedure found optimal trade-offs between design and control decisions, based on process dynamics and advanced control. The innovation embedded in the control optimization approach, suggested a two-stage problem decomposition leading to an important reduction of the original problem size and complexity (mass balances plus optimization). Integration of design and control is expected to reach broad impact on high-performance systems, operated close to their limits.

4. CONCLUSSIONS

An innovative lubricating system for internal combustion engines, which considers continuous supply of lubricant precursors, has been proposed. The operating region is defined by a compromise among flows, make-up and between the oil pan and the engine, and the required tribofilm width that ensures proper lubricating of the engine. The optimum operating point has been located as a compromise between the two flows, named $q(t)$ and $u(t)$ and the excess variable θ_A. Additionally, using the optimal control methodology, feasible tracks for the regulation of the make-up flow have been obtained; all depending on the composition of the lubricant coming from the oil pan to the engine, ρ_{AC}. This analysis is an example of the simultaneous issues of design and control of dynamic processes.

ACKNOWLEDGEMENTS

Authors gratefully thank CONACYT for sponsorship and grants, also thank CIC-Universidad Michoacana de San Nicolás de Hidalgo for funding of these studies.

REFERENCES

V.M. Alekseev. *Optimal Control*. New York, Springer Science + Business Media, LLC, 2013, p.p. 250-275.

R. Aris, C. Truesdell. Prolegomena to the rational analysis of systems of chemical reactions. *Process Systems Engineering*, vol. 1, no. 1, pp. 149–169, 1999.

N.A. Bhore, M.T. Klein, K.B. Bischoff. The Delplot Technique: A New Method for Reaction Pathway Analysis. *Industrial & Engineering Chemistry Research*, vol. 29, no. 2, pp. 313–316, 1990.

D. Constales, G.S. Yablonsky, G.B. Marin. Predicting kinetic dependences and closing the balance: Wei and Prater revisited. *Chemical Engineering Science*, vol. 123, pp. 328–333, 2015.

S. Domínguez-García, L. Béjar-Gómez, R. Huirache-Acuña, J. Lara-Romero, and R. Maya-Yescas. Delumping strategy to infer lubricating reaction pathways in internal combustion engines. *International Journal of Chemical Reactor Engineering*, vol. 18, Art. 1, 2020.

S. Domínguez-García, C.E. Aguilar-Ramírez, L. Béjar-Gómez, and R. Maya-Yescas. Mass balance of the tribofilm in lubricated systems. *Tribology International*, vol. 155, Art. 106757, March 2021.

L. Ma, J. Luo. Thin film lubricating in the past 20 years. *Friction*, vol. 4, no. 4, p.p. 280–302, 2016.

A. Malcolm, J. Polan, L. Zhang, B.A. Ogunnaike, A.A. Linninger. Integrating systems design and control using dynamic flexibility analysis. *AIChE J*, vol. 53, no. 8, p.p. 2048-2061, 2007.

J. Wei. Structure of complex chemical reaction systems. *Industrial & Engineering Chemistry Fundamentals*, vol. 4, no. 2, pp. 161–167, 1965.

B. Zhao, X.D. Dai, Z.N. Zhang, Y.B. Xie, A new numerical method for piston dynamics and lubricating analysis. *Tribology International*, vol. 94, February, pp. 395–408, 2016.

Appendix A. TRACKS TO TRADE-OFF STEADY STATE

A simple way to model chemical reactions in lubricating system is assuming pseudo-first order kinetics (Domínguez-García, 2020), which does group apparent kinetic constants (Domínguez-García, 2020; Constales et al., 2015; Aris, 1999; Bhore et al., 1990; Wei, 1965). So, for the case of the tribofilm formation the apparent kinetic constant is κ_A, this constant groups the surface area available for the reaction, the temperature, the mass fraction of oil that contains the precursors and the contribution of the tribological effect. So, from the above assumptions, kinetics of tribofilm formation is equal to the apparent kinetic constant times the mass of lubricant precursors m_A available in the lubricant blend (A.1). Besides, it is no difficult to deduce from the law of conservation of mass that removal of deposited mass due tribofilm wear is equal to its first order constant κ_F times the deposited tribofilm mass m_F (A.2).

$$|r_A = \kappa_A \cdot m_A \tag{A.1}$$

$$|r_F = \kappa_F \cdot m_F \tag{A.2}$$

These rates are introduced to model the two main reactions (Fig. 1), and all the expressions are squeezed together to develop the classical mass balances (A.3, A.4) for tribofilm precursors (*A*) and tribofilm deposited on the rubbing surfaces (*F*), bases of the model used (Domínguez-García et al., 2021).

$$\frac{dm_A}{dt} = u \cdot (\rho_{A\,C} - \rho_{A\,M}) - V_M \cdot |r_A \tag{A.3}$$

$$\frac{dm_F}{dt} = V_M \cdot (|r_A - |r_F) \tag{A.4}$$

